Remote sensing image registration based on Gaussian-Hermite moments and pseudo-RANSAC algorithm

Li, Ying; Li, Fangyi; Yang, Kaixing ; Price, Christopher; Shen, Qiang

Published in:
Remote Sensing Letters

DOI:
10.1080/2150704X.2017.1364874

Publication date:
2017

Citation for published version (APA):
Li, Y., Li, F., Yang, K., Price, C., & Shen, Q. (2017). Remote sensing image registration based on Gaussian-Hermite moments and pseudo-RANSAC algorithm. *Remote Sensing Letters*, *8*(12), 1163–1172. https://doi.org/10.1080/2150704X.2017.1364874

Remote Sensing Image Registration Based on Gaussian-Hermite Moments and the Pseudo-RANSAC Algorithm

Ying Li[a] and Fangyi Li[a,b] and Kaixing Yang[a] and Chris Price[b] and Qiang Shen[b]

[a]School of Computer Science and Engineering, Northwestern Polytechnical University, Shaanxi, Xi'an 710129, China;
[b]Department of Computer Science, Institute of Mathematics, Physics and Computer Science, Aberystwyth University, SY23 3DB Aberystwyth, U.K

ARTICLE HISTORY
Compiled July 25, 2017

ABSTRACT
This study deals with an important issue that is often encountered with the registration of remote sensing images which are obtained at different times and/or through inter/intra sensors. Remote sensing images may differ significantly in gray-level characteristics and contrast, among other aspects. Thus, it may be difficult to apply directly area-based approaches which are dependent on image intensity values. In this work, a novel approach for automatic image registration based on Gaussian-Hermite moments and the Pseudo-RANSAC algorithm is proposed. The problem of intensity difference commonly incurred in multi-temporal or multimodal remote sensing image registration is tackled using features that are invariant to intensity mapping during the feature point matching process. In particular, the feature points are herein represented by a range of newly introduced Gaussian-Hermite moments, and the corresponding feature points in a certain reference image are sought with the Euclidean distance measure. Moreover, an improved RANdom SAmple Consensus (RANSAC) algorithm is presented, reducing computational time complexity while improving performance in stability and accuracy. The final warping of images according to their refined feature points is conducted with bilinear interpolation. The proposed approach has been successfully applied to register synthetic and real remote sensing images, demonstrating its efficacy with systematic experimental evaluations.

KEYWORDS
remote sensing, Gaussian-Hermite moments, Pseudo-RANSAC, image registration.

1. Introduction

The rapid development of remote sensing technology has led to the availability of rich data in the form of remote sensing images, providing substantial information that is useful for global weather change research, environmental monitoring and assessment, resource survey and disaster prevention, amongst many others. A variety of image processing and analysing technologies in remote sensing have been developed. A common and important underpinning technique for this is image registration, which plays an indispensable role in numerous remote sensing applications. Image registration aims to analyse two or more different images of the same scene, taken at different

Corresponding author: Ying Li. Email: lybyp@nwpu.edu.cn

times, by different sensors, or from different viewing angles. It is a key stage in the development of image modelling and analysis systems for applications such as image fusion (Li et al. 2016), change detection and super-resolution imaging (Vakalopoulou et al. 2016). In image registration, a certain reference image and other sensed images are to be matched. The main goal of the registration is to warp the sensed images into the coordinate system of the reference image, in order to ensure that the corresponding coordinate points between them fit the same coordinate location.

The feature-based image registration approaches (Li et al. 2009) are commonly used due to their good performance of high accuracy. They usually extract prominent distinctive features that are possibly uniformly spread over the images and readily detectable. Significant regions, lines and points are well known as descriptive features (Jiang and Shi 2016; Li, Cui, and Han 2012). In particular, features based on point localization are perhaps the most commonly used for image registration procedures, as they can provide a highly effective parametric description of the correspondence based on just point coordinates. Following this approach, in general, feature points are first extracted from both the reference image and the sensed image. Then, a robust feature description is constructed in terms of each feature, with the resulting feature descriptors to be matched. To improve the robustness and accuracy of this process, in order to minimize mismatching, the RANdom SAmple Consensus (RANSAC) algorithm (Fischler and Bolles 1981), the most commonly used approach, is to eliminate outliers from the set of initial pairs of feature descriptions.

Unfortunately, the RANSAC algorithm works in an iterative manner, which leads to the issue of low efficiency. Since the initial feature points in the RANSAC iterative process are selected randomly, the resulting transformation models may be unstable. Hence, a novel Pseudo-RANSAC algorithm with preprocessing is proposed in this letter to address this problem. In addition, note that moments and functions of moments can successfully separate image features. They have found wide applications in the field of image processing. In particular, Gaussian-Hermite moments (GHMs) have been widely used in various image processing tasks (Yang and Dai 2012; Yang et al. 2017), such as target detection, image recognition and classification, and image reconstruction. Many applications confirmed that Gaussian-Hermite moments have a potential capability in feature representation (Wang, Wu, and Dai 2007). Inspired by this observation, this letter also introduces the Gaussian-Hermite moments as the descriptors of feature points for remote sensing image registration, with an aim to further improve performance of the proposed image registration algorithm.

2. Methodology

This section presents a novel image registration approach, which constructs the Gaussian-Hermite moments as feature descriptors and utilizes the Pseudo-RANSAC algorithm to obtain the refined matching pairs for building the transformation model. The flow of the proposed approach is illustrated in Figure 1.

Before outlining the proposed method, it is necessary to declare that the reference image and the sensed image are assumed to be attained at the same or approximately equal spatial resolution. Given the reference image and the sensed image, two sets of Feature Points (FPs) are extracted automatically by utilizing the Harris_Laplacian (Mikolajczyk 2004) corner detector algorithm, which has proven to be able to extract interesting points that are invariant to scale, rotation and translation as well as robust to illumination changes. Each FP is then descripted via the feature

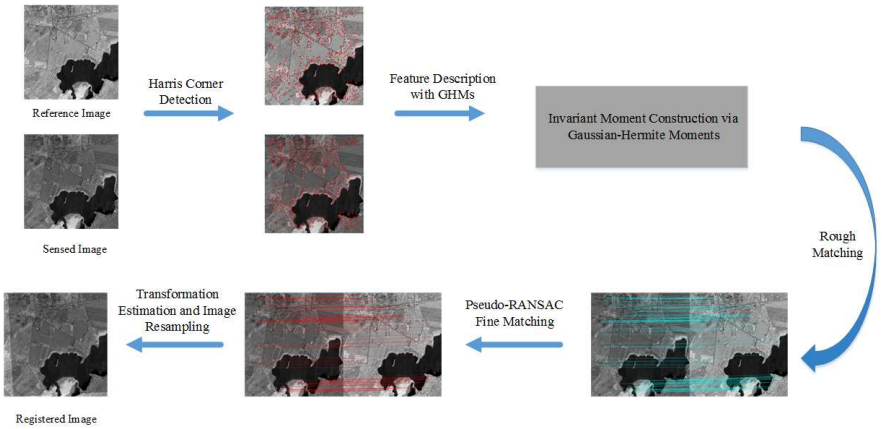

Figure 1. Workflow of the proposed approach

invariants of Gaussian-Hermite Moments (GHM) of five orders in both the reference image and the sensed image space to construct the invariant feature vectors. Then the feature vectors from the sensed image space need to be matched with those from the reference image space. The Euclidean distance-based measure is employed as the rough matching criterion to determine the initial matching point (MPs) pairs, resulting in the establishment of correspondence of the selected FPs. It is necessary to refine the MPs in order to build a spatial transformation model that maps the sensed image to the reference image. The proposed Pseudo-RANSAC algorithm is herein applied to achieve fine matching. Moreover, the affine transformation model can also be estimated accordingly after the termination of algorithm. Finally, the sensed image is transformed to the reference image space based on the final transformation model, and then resampled by using the bilinear interpolation technique. Bilinear interpolation is chosen here because of its fast speed with moderate accuracy, while GHM descriptors already help to achieve a high performance in terms of the overall accuracy.

The two contributions to the proposed image registration approach are Gaussian-Hermite moments feature descriptor and Pseudo-RANSAC algorithm for image registration, which are illustrated in the following, respectively.

2.1. *Invariant Feature Construction via Gaussian-Hermite Moments*

Intensity changes in images arise from surface discontinuities or from reflectance or illumination boundaries. Such changes all have the property that they are spatially localized. Therefore, an edge represents specific spatial information in an image. Usually, the gradient operator is locally defined and normally used to detect the edge where pixels belong to the object boundaries. Such edge features can depict the distribution of the boundary pixels in the image.

The difference-of-Gaussian (DoG) manipulated in the images presents a distinctive image of an edge for both the reference image and the sensed image. It is obtained by subtracting two successive smoothed images (Mikolajczyk 2004). As the smoothed scale factor (σ_0) becomes larger, the image is increasingly blurred. The DoG function also provides a close approximation to the scale-normalized Laplacian of the Gaussian, but it can significantly accelerate the computation process (Lindeberg 1994). The DoG is given as follow:

$$D(x, y, \sigma_0) = (G(x, y, k\sigma_0) - G(x, y, \sigma_0)) * I(x, y) \quad (1)$$

where $I(x, y)$ is the source image, $G(x, y, \sigma_0)$ is the Gaussian kernel and the k is fixed to 1.6 empirically. The asterisk represents the convolution manipulation.

Now that the original images and the DoG images have been obtained, they can be used to compute the Gaussian-Hermite moments in both the reference and sensed image space. The independent and complete eighteen feature invariants (i.e., $\Phi_i, i = (1, 2, \ldots, 18)$) of Gaussian-Hermite moments up to the fifth order can be derived using Flussers theory (Flusser, Zitova, and Suk 2009; Yang et al. 2011, 2017) and calculated with fast algorithm (Hosny 2012):

- Second order: Φ_1;
- Third order: Φ_2, Φ_3, Φ_4, Φ_5, Φ_6;
- Fourth order: Φ_7, Φ_8, Φ_9, Φ_{10}, Φ_{11};
- Fifth order: Φ_{12}, Φ_{13}, Φ_{14}, Φ_{15}, Φ_{16}, Φ_{17}, Φ_{18}.

The invariant features consist of the Gaussian-Hermite moments M_{mn} of order $(m + n), m = 0, 1, \ldots, 5, n = 0, 1, \ldots, 5$. For example, Φ_1 in the second order group can be decomposed such that $\Phi_1 = M_{20} + M_{02}$, where M_{20} and M_{02} are the second order GHM. The $M_{mn}, m = 0, 1, \ldots, 5, n = 0, 1, \ldots, 5$ is normalized by:

$$M_{mn} = \frac{M_{mn}}{M_{00}} \quad (2)$$

This normalisation with zero-order moment M_{00} is employed to eliminate the adverse effect involved in the implementation of the construction of GHM invariant features to image scaling (details can be referred to (Yang et al. 2017)). Note that these employed features are invariant to image rotation, translation and scaling, which is essential to image registration for the remote sensing images. The detailed definition of GHM (e.g., $M_{mn}, m = 0, 1, \ldots, 5, n = 0, 1, \ldots, 5$) and its composition of invariant features (i.e., $\Phi_i, i = (1, 2, \ldots, 18)$) is beyond the scope of this paper but can be found in (Yang et al. 2011, 2017) and hence, omitted here due to limited space.

A moment vector is generated by computing the above Gaussian-Hermite invariant moments in a region of radius $15\sigma_0$ (σ_0 is typically set in the range of 0 to 1) around the location of the feature point. For each feature point, the moment vector $V_i\sigma_j$ is computed on the original image and different-of-Gaussian image in the reference and/or the sensed image space

$$V_{i\sigma_j} = [\Phi_1\Phi_2 \ldots \Phi_{17}\Phi_{18}](1 \leq i \leq 2, 1 \leq j \leq 5) \quad (3)$$

where i represents the two images in the reference and/or the sensed image space, and the five scale parameters $\sigma_j(1 \leq j \leq 5)$ were successively fixed to 0.1, 0.2, 0.4, 0.7 and 1.2, which are set on the basis of empirical investigations. Therefore, the feature vector of each feature point is constructed by combining all the moment vectors that are computed in different scales and image space:

$$V = [V_{1\sigma_1} \ldots V_{1\sigma_5} V_{2\sigma_1} \ldots V_{2\sigma_5}] \quad (4)$$

2.2. *Pseudo-RANSAC Algorithm for Estimation of Model Parameters*

The proposed Pseudo-RANSAC algorithm with preprocessing is presented in this section. The low efficiency of the original RANSAC algorithm may be caused by its iterative runs on the random selected initial sets of matching pairs. Inspired by this, a

set of selected pairs with high stability is input to the RANSAC procedure. In order to generate these stable point pairs, a preprocessing of Delaunay triangulation is involved to work with the Pseudo-RANSAC algorithm as an integrated part. The preprocessing and the method of selection of initial matching pairs for RANSAC procedure are illustrated in the following, respectively.

2.2.1. Preprocessing for initial matching pairs

To obtain the best transformation model using the RANSAC algorithm requires many runs, particularly when the proportion of inliers in the data is low. This does not only incur extra computational cost and low efficiency, but leads to non-convergence to the optimal solution. Hence, in order to obtain a more stable subset, we utilise the spatial topological relationship to screen the initial matching pairs and to reduce the outliers as much as possible at the beginning.

The Delaunay triangulation (Bhattacharya and Gavrilova 2012), which is commonly used to subdivide or interpolate on a given set of points, is employed to subdivide the set of initial matching pairs, resulting in screening the set. Given the triangle topological structures, each initial matching pair in the triangle net is determined as to whether it belongs to a new dataset as follows.

Suppose P and P$'$ are a pair of initial matching points, which is represented as triangle vertex in its Delaunay triangle topological structures, respectively. N_0 vertices and N_0' vertices are adjacent to P and P$'$. There are m pairs of the initial matching set among the adjacent points. The vertices which are adjacent to P are denoted P_1,P_2,...,P_m, and the vertices which are adjacent to P$'$ are denoted P'_1,P'_2,...,P'_m. N denotes the maximum between N_0 and N_0'.

If $\beta = \frac{m}{N} > \beta_0$, construct a vector $\boldsymbol{V} = [v_1, v_2, ..., v_m]$ and $v_i, i = 1, 2, \ldots, m$ is demoted as:

$$v_i = \frac{\|P - P_i\|}{\|P' - P'_i\|} \tag{5}$$

$\|P - P_i\|$ represents the Euclidean distance between a pair of features which are mapped by a pair of vertices. σ is the variance of the vector $\boldsymbol{V}$. If $\sigma < \sigma_0$, the geometric constraint between this pair is met, and then it belongs to one of elements of the new matching pair set S. Finally, according to the above method, check all of the pairs in the initial matching set, and add the pairs which meet these two conditions to the new set. The obtained subset S is regarded as the input to the Pseudo-RANSAC algorithm.

2.2.2. Pseudo-RANSAC Algorithm

A part of outliers could be eliminated using the Delaunay triangulation for initial matching set. It delivers a moderately stable subset. Then we refine the elements of subset utilising the Pseudo-RANSAC algorithm to gain stable inliers, and estimate transform matrix model in the meanwhile.

After the Delaunay triangulation, we re-calculate every variance σ of each vector $\boldsymbol{V}$, and save the corresponding pair as well as its adjacent pairs in the set MP. Then we sort the variance and select the set MP corresponding to the minimum variance. If the number of pairs in set MP is less than three, then we select the set corresponding to the second minimum variance. Assume that the selected set is denoted MP_k corresponding to the variance σ_k , the Pseudo-RANSAC algorithm is presented as follows.

Algorithm 1 Pseudo-RANSAC algorithm
Input: The set MP_k , the distance threshold ϵ, the maximum sampling times $N_{\max}$
Output: Transform matrix H
1: **for** $t = 1 : N_{\max}$ **do**
2: Initialize the set of inliers Q=MP_k;
3: Select three pairs in the set Q, which are non-collinear spatially;
4: Estimate the spatial transformation model H in terms of selected pairs;
5: Select the i^{th} candidate pair (P_i,P'_i) to determine whether it is an inlier or not. If a pair of points (P_i,P'_i) satisfy $\|P_i - H\,(P'_i)\| \leq \epsilon$, then they are selected to the inliers set Q;
6: **end for**
7: Select the set which has the largest number of refined pairs during the iteration, and then calculate the model parameters for constructing the transformation matrix H.
8: **return** Transform matrix H.

3. Experimental Evaluation and Discussion

In this section, three sets of experiments are implemented to evaluate the performance of the proposed Gaussian-Hermite Moments (GHM) feature descriptor and the Pseudo-RANSAC algorithm. Firstly, The proposed feature descriptor is compared with three classical methods: SIFT (Fan et al. 2013), Pseudo Zernike Moment (PZM) (Xia et al. 2007) and KAZE (Alcantarilla, Bartoli, and Davison 2012). All these methods adopt the standard RANSAC procedure to refine the matching points. In particular, the PZM descriptor constructs feature descriptions for the feature points which are extracted by the Harris_Laplacian method in the same way as the proposed algorithm does. Moreover, the performance of registration on real satellite images is investigated by varying the order of GHM for constructing GHM invariant features. The last comparative experiment between the standard RANSAC and the proposed Pseudo-RANSAC method is carried out based on SIFT, KAZE and GHM features.

3.1. *Data and experimental set-up*

A pair of synthetic remote sensing images are used to test the performance of GHM feature description against the other three features. The sensed image is modified from the Landsat TM (Band 7) satellite image by transforming the corresponding reference image using preset affine transformation model AT= $\begin{bmatrix} 0.85+\cos 0.3 & -\sin 0.3 & 100 \\ \sin 0.3 & 0.85+\cos 0.3 & 100 \\ 0 & 0 & 1 \end{bmatrix}$. The size of images is 600×600 pixels.

The comparison of the Pseudo-RANSAC algorithm over the standard RANSAC is tested on two pairs of real satellite images. One is a set of two 400×400 hyperspectral images and another is a set of two 400×400 Landsat TM Band 5 and Band 3 images. The SIFT/KAZE features-based registration methods are also implemented to demonstrate the flexibility of the usage of Pseudo-RANSAC algorithm.

Some other parameters are set as per the empirical values. In the Harris corner detector algorithm, the empirical value $k = 0.04$. The threshold for corner determination is $R = 5000$. In the preprocessing of Pseudo-RANSAC algorithm, two thresholds for picking pairs into subset S are: $\beta_0 = 0.25$, $\sigma_0 = 0.50$. Otherwise it shares the same

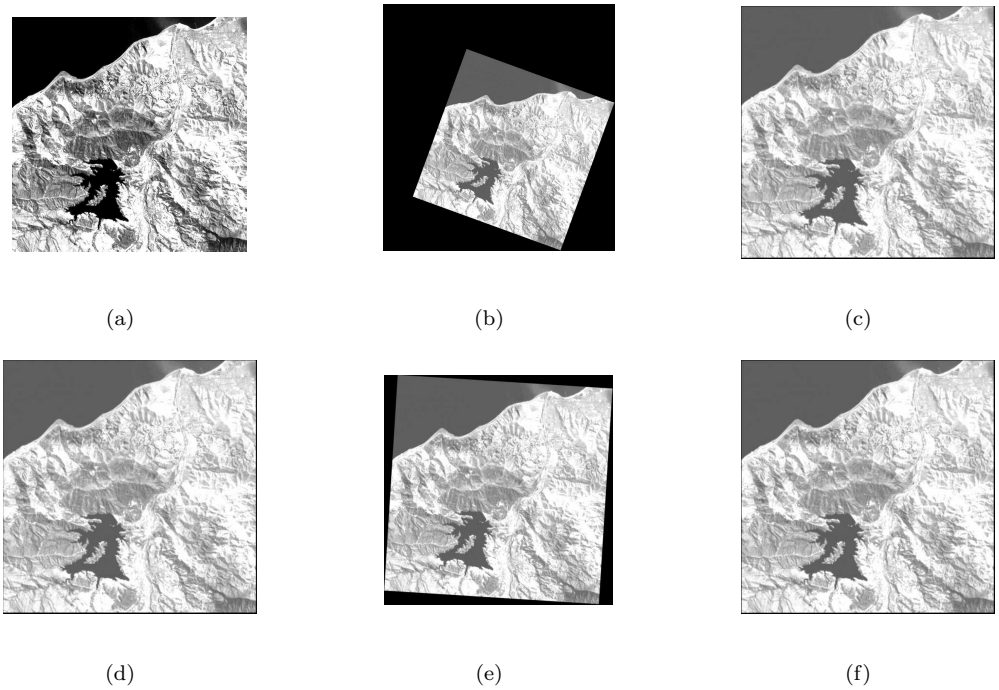

Figure 2. Image registration for synthetic image. (a) Reference image. (b) Sensed image. (c) Aligned image based on GHM. (d) Aligned image based on SIFT. (e) Aligned image based on PZM. (f) Aligned image based on KAZE.

parameters as basic RANSAC as follows: the distance threshold ϵ is fixed to 0.0002, confidence coefficient $p = 0.99$, and the proportion of inliers $\omega = 0.4$, so that the maximum sampling times is defined as $N_{\max} = \lg(1-p) / \lg(1-\omega^4)$.

The accuracy of the proposed and comparative approaches is estimated by using the Root Mean Square Error (RMSE) over every refined MPs pairs. The lower RMSE is, the better performance of image registration will be.

3.2. *Results and discussion*

3.2.1. Comparison on different features

The results of the proposed GHM feature and comparative features are shown in Figures 2. The quantitative evaluation is shown in Table 1, which contains the numbers of initial matched pairs (IMPs) and refined matched pairs (RMPs), and RMSE. Note that the better performance is shown in bold in all of the following comparative tables.

The registration on synthetic images demonstrates the performance of geometric correction of each image registration algorithm, on artificially simulated images. The synthetic sensed image is transformed using affine transform models, which include scale, rotation and translation transform. These transformations are very common in remote sensing images, especially for the images captured by different sensors. As can be seen the resultant registered images in Figure 2 (c-f), the proposed image registration algorithm with GHM rectifies the geometric transformation better than SIFT, KAZE and PZM-based image registration methods. In other words, the original reference images can be better recovered with the proposed image registration algorithm. This is also validated by the quantitative RMSE values shown in Table 1. The

Table 1. Quantitative comparison of registration algorithm with proposed GHM feature and other three features

Features for Registration	No. of IMPs	No. of RMPs	RMSE(pixels)
SIFT	3531	3519	29.4753
KAZE	14	14	29.8286
PZM	25	9	173.7677
GHM	36	9	**14.4565**

Table 2. Quantitative comparison of GHM features constructed with different orders of Gaussian-Hermite moments

Image Data and Size(pixels)	Maximum Order of GHMs	No. of RMPs/IMPs	RMSE(pixels)	Time(s)
AVIRIS (Band 39) 250×250	5th order	32/45	**0.6246**	8.0586
	4th order	31/43	0.7044	7.4765
	3rd order	30/44	0.7745	7.0745
Landsat TM (Band 4) 400×400	5th order	26/26	**0.1898**	49.0561
	4th order	21/21	71.9515	44.2369
	3rd order	20/22	93.3711	40.5637
Landsat TM (Band 5) 512×512	5th order	28/34	**0.7203**	74.6671
	4th order	29/39	39.2514	68.4713
	3rd order	25/35	45.2150	62.9739

proposed method has achieved the least error. In particular, compared with another moment-based feature descriptor (i.e., PZM-based method), GHM did significantly much better than PZM in both visual assessment and quantitative evaluation. Moreover, the proposed method outperforms the SIFT method even though the number of matched pairs of feature points is prominently less than the latter. These results clearly demonstrate the potential ability of the proposed algorithm in keeping invariant under scale, rotation and translation transformation in remote sensing images.

3.2.2. Comparison on GHM orders for invariant feature construction

Three pairs of real satellite images as given in Table 2 are investigated regarding the impact of this work upon registration precision and running time, by varying the order of GHM for the construction of invariant features. The main body of the experimental study is based on the fifth order GHM. Here, the GHM invariant features are constructed with up to the third, the fourth and the fifth order, respectively.

The results listed in Table 2 clearly indicate that the GHM invariant features constructed with a higher order outperform those with lower orders. The registration accuracy can achieve sub-pixel precision with use of any of the three orders for image pair 1. For image pairs 2 and 3, the algorithm may lose the capability of registration which corrects geometrically the change of the sensed image based on the reference image. In particular, the performance with the third or fourth order is much poorer. Since the number of invariant features generated with lower orders is fewer (11 invariants for the fourth order and 6 invariants for the third order), the time-consumption is a little bit less than the use of 18 invariant features while the fifth order is employed. From the practical viewpoint, however, it is necessary, and more important, to achieve reasonable and accurate registration for remote sensing images. This confirms the desirable design choice of the fifth order in the present work.

3.2.3. Comparison with standard RANSAC algorithm

Table 3 illustrates the performance of comparison results of the proposed Pseudo-RANSAC and the standard RANSAC algorithm for model parameter estimation using

Table 3. Comparative performance of RANSAC and Pseudo-RANSAC algorithms based on three different features

	Methods	No. of RMPs/IMPs	RMSE(pixels)	Time(s)
SIFT Features				
Hyper-spectral images	RANSAC	209/221	0.3547	8.93
	Pseudo-RANSAC	215/221	**0.3175**	**5.70**
Landsat TM images	RANSAC	161/183	0.3557	8.05
	Pseudo-RANSAC	168/183	**0.3236**	**5.24**
KAZE Features				
Hyper-spectral images	RANSAC	18/19	0.3039	2.34
	Pseudo-RANSAC	17/19	**0.2653**	**1.23**
Landsat TM images	RANSAC	18/21	0.3898	3.04
	Pseudo-RANSAC	18/21	**0.3214**	**2.14**
Gaussian-Hermite moments Features				
Hyper-spectral images	RANSAC	76/82	**0.2388**	5.76
	Pseudo-RANSAC	76/82	**0.2388**	**3.89**
Landsat TM images	RANSAC	73/79	0.2297	6.32
	Pseudo-RANSAC	72/79	**0.2036**	**4.04**

SIFT, KAZE and GHM features, respectively. From the table we can see that both the standard RANSAC and the Pseudo-RANSAC can achieve good results. The error is at sub-pixel level, based on whichever features they exploited. In particular, Pseudo-RANSAC algorithm with preprocessing shows outperformance on not only accuracy, but time-consumption for computation of the transformation model. The main reason is that through the improvements on RANSAC, quite a lot of outliers are rejected by constructing a spatial topological relationship among matching pairs. Moreover, the selection of a subset with higher space consistency and continuity for initial pairs of the Pseudo-RANSAC helps to avoid the instability of random selection, which eventually speeds up the process significantly.

Collectively, the performance of the proposed image registration algorithm which combine Gaussian-Hermite moment features and the Pseudo-RANSAC algorithm is also demonstrated in Table 3. It is indicated that local features are extracted and described more precisely by utilizing the GHM feature descriptor, which results in strong capability of feature representation. High accuracy is again achieved by the Pseudo-RANSAC algorithm since it reduces the number of iteration and perhaps thus decreases time-consuming effectively.

4. Conclusion

This letter presents a novel method for addressing the image registration of remote sensing images. Two significant contributions are demonstrated and employed in the framework of the feature-based image registration. Gaussian-Hermite moments of order five are utilized to construct feature vectors, which are invariant to image scaling, rotation and translation transformation. It has been shown that the accuracy is much higher than that of the other three comparable classical features. At the stage of fine matching, an improved algorithm of outlier rejection and estimation of model parameters (i.e., Pseudo-RANSAC algorithm) is proposed to refine the correspondences, which reduces the computational complexity significantly compared with the standard RANSAC algorithm. The experimental evaluation illustrates the prior performance on the effectiveness and efficiency of the proposed work.

Acknowledgement(s)

This work was supported by National Key Research and Development Program No. 2016YFB0502502. The authors would like to thank Dr. B. Yang for his help during this work. The authors are also grateful to the anonymous reviewers for their constructive comments which have helped improve this work.

References

Alcantarilla, Pablo Fernández, A Bartoli, and A J Davison. 2012. *KAZE Features*, 214–227. Berlin, Heidelberg: Springer Berlin Heidelberg.

Bhattacharya, Priyadarshi, and M Gavrilova. 2012. "Improving RANSAC Feature Matching with Local Topological Information." In *2012 Ninth International Symposium on Voronoi Diagrams in Science and Engineering*, June, 17–23.

Fan, Bin, C Huo, C Pan, and Q Kong. 2013. "Registration of Optical and SAR Satellite Images by Exploring the Spatial Relationship of the Improved SIFT." *IEEE Geoscience and Remote Sensing Letters* 10 (4): 657–661.

Fischler, MA, and R Bolles. 1981. "Random sample consensus: a paradigm for model fitting with applications to image analysis and automated cartography." *Communications of the ACM* 24 (6): 381–395.

Flusser, Jan, B Zitova, and T Suk. 2009. "Moments and moment invariants in image analysis." In *International Conference on Image Processing*, 1–36.

Hosny, Khalid M. 2012. "Fast computation of accurate Gaussian–Hermite moments for image processing applications." *Digital Signal Processing* 22 (3): 476–485.

Jiang, Jie, and X Shi. 2016. "A Robust Point-Matching Algorithm Based on Integrated Spatial Structure Constraint for Remote Sensing Image Registration." *IEEE Geoscience and Remote Sensing Letters* 13 (11): 1716–1720.

Li, Qiaoliang, G Wang, J Liu, and S Chen. 2009. "Robust Scale-Invariant Feature Matching for Remote Sensing Image Registration." *IEEE Geoscience and Remote Sensing Letters* 6 (2): 287–291.

Li, Ying, Y Cui, and X Han. 2012. "Optical Image and SAR Image Registration Based on Linear Features and Control Points." *ACTA AUTOMATICA SINICA* 28 (12): 1968–1974.

Li, Ying, F Li, B Bai, and Q Shen. 2016. "Image fusion via nonlocal sparse K-SVD dictionary learning." *Applied Optics* 55 (7): 1814–1823.

Lindeberg, Tony. 1994. "Scale-space theory: A basic tool for analyzing structures at different scales." *Journal of applied statistics* 21-22: 225–270.

Mikolajczyk, Krystian C Schmid. 2004. "Scale & affine invariant interest point detectors." *International journal of computer vision* 60 (1): 63–86.

Vakalopoulou, Maria, K Karantzalos, N Komodakis, and N Paragios. 2016. "Graph-Based Registration, Change Detection, and Classification in Very High Resolution Multitemporal Remote Sensing Data." *IEEE Journal of Selected Topics in Applied Earth Observations and Remote Sensing* 9 (7, SI): 2940–2951.

Wang, Lin, Y Wu, and M Dai. 2007. "Some Aspects of Gaussian-Hermite Moments in Image Analysis." In *Third International Conference on Natural Computation*, Vol. 2, 450–454.

Xia, Ting, H Zhu, H Shu, P Haigron, and L Luo. 2007. "Image description with generalized pseudo-Zernike moments." *J. Opt. Soc. Am. A* 24 (1): 50–59.

Yang, Bo, and M Dai. 2012. "Image reconstruction from continuous Gaussian-Hermite moments implemented by discrete algorithm." *Pattern Recognition* 45 (4): 1602–1616.

Yang, Bo, J Kostková, J Flusser, and T Suk. 2017. "Scale invariants from Gaussian–Hermite moments." *Signal Processing* 132: 77–84.

Yang, Bo, G Li, H Zhang, and M Dai. 2011. "Rotation and translation invariants of Gaussian-Hermite moments." *Pattern Recognition Letters* 32 (9): 1283–1298.